Journal of the Optical Society of America A
OPTICS, IMAGE SCIENCE, AND VISION

Degree of polarization in the focal region of a lens

XINYING ZHAO,[1,2] TACO D. VISSER,[1,2,3,*] AND GOVIND P. AGRAWAL[3,4]

[1]Department of Physics and Astronomy, Vrije Universiteit, Amsterdam, NL-1081HV, The Netherlands
[2]School of Electronics and Information, Northwestern Polytechnical University, Xi'an, 710129, China
[3]Department of Physics and Astronomy, University of Rochester, Rochester, New York 14627, USA
[4]The Institute of Optics, University of Rochester, Rochester, New York 14627, USA
*Corresponding author: tvisser@nat.vu.nl

Received 18 June 2018; revised 14 July 2018; accepted 15 July 2018; posted 16 July 2018 (Doc. ID 335497); published 8 August 2018

We examine the 3D distribution of the degree of polarization (DOP) in the focal region of a thin paraxial lens. Analytic expressions for the case of a focused Gaussian–Schell model beam are derived. These show that the DOP satisfies certain spatial symmetry relations. Furthermore, its value varies strongly in the vicinity of the geometrical focus, and its maximum, which need not occur at the focus, can be significantly higher than that of the incident beam.

OCIS codes: (030.1640) Coherence; (260.2110) Electromagnetic optics; (260.5430) Polarization; (050.1960) Diffraction theory; (050.1965) Diffractive lenses.

https://doi.org/10.1364/JOSAA.35.001518

1. INTRODUCTION

The state of polarization (SOP) of an electromagnetic beam [1] is a fundamental quantity that determines how it behaves on scattering [2] and how it propagates through a birefringent medium. When the beam is partially polarized, the SOP is furthermore quantified by the degree of polarization (DOP), which is defined as the ratio of the spectral density of the portion of the field that is fully polarized and the total spectral density. Both the SOP and the DOP are local quantities that may vary significantly from point to point. Furthermore, they both typically change on propagation, even when that propagation is through free space [3–5].

It is well known that the focusing action of a lens can drastically change the properties of a stochastic wave field, such as the intensity distribution [6], the spectral degree of coherence [7], and its transverse coherence length [8]. Although the DOP is widely applied, for example, as a gating technique in scattering [9], as a diagnostic tool in material science [10], in optical coherence tomography [11], and in remote sensing [12], the effect of a lens on the DOP of a random beam has until now received scant attention. Notable exceptions are [13,14]. In the latter study, it was found that focusing a completely unpolarized 3D field changes its polarization properties.

In a previous study by the present authors, it was predicted that focusing a partially polarized beam (i.e., a 2D field) can strongly increase the DOP in the focal plane, and that spatial filtering in a 4f setup can be used to control this effect [15].

In this paper, we chart the 3D distribution of the DOP in the focal region of a thin lens. Within the validity of the paraxial approximation, we derive explicit expressions for the DOP of a Gaussian–Schell model beam and show that it satisfies certain spatial symmetry properties. The DOP has a nontrivial structure, and its maximum need not occur at the geometrical focus.

In our analysis, the DOP is calculated from knowledge of the so-called cross-spectral density matrix, which describes the second-order coherence properties of a beam-like field [16]. In an experiment [17,18], the DOP, denoted as $P(\mathbf{r},\omega)$, can be inferred from the Stokes parameters through the relation [19]

$$P(\mathbf{r},\omega) = \frac{\sqrt{S_1^2(\mathbf{r},\omega) + S_2^2(\mathbf{r},\omega) + S_3^2(\mathbf{r},\omega)}}{S_0(\mathbf{r},\omega)}. \qquad (1)$$

Here, the symbols $S_i(\mathbf{r},\omega)$, with $i = 0,1,2,3$, represent the spectral Stokes parameters at position $\mathbf{r}$ at frequency ω. The DOP is bounded by 0 and 1. These limits correspond to a completely unpolarized beam and a fully polarized beam, respectively. For intermediate values, the beam is said to be partially polarized.

2. PARAXIAL FOCUSING

Consider first a partially coherent scalar beam that propagates close to the z axis and that is focused by a thin paraxial lens of focal length f. Let $U^{(\mathrm{in})}(\boldsymbol{\rho},\omega)$ denote the field at the entrance plane of the lens at a transverse position $\boldsymbol{\rho} = (x,y)$. Then, the field distribution in the exit plane (ep) immediately behind the lens is given by the expression (Sec. 5.1.3, [20])

$$U^{(\mathrm{ep})}(\boldsymbol{\rho},\omega) = U^{(\mathrm{in})}(\boldsymbol{\rho},\omega)A(\boldsymbol{\rho})\exp[-jk\rho^2/2f]. \tag{2}$$

Here, the exponent represents the phase function of the lens, with the wavenumber $k = 2\pi/\lambda = \omega/c$, where λ denotes the wavelength, and c is the speed of light. The pupil function $A(\boldsymbol{\rho})$ takes on the value 1 for points inside the aperture and 0 elsewhere. Within the framework of Fresnel diffraction, the field at an arbitrary position $(\boldsymbol{\rho}, z)$ behind the lens becomes (Sec. 4.2, [20])

$$U(\boldsymbol{\rho},z,\omega) = \frac{\exp[jk\rho^2/2z]}{j\lambda z}e^{jkz}\iint_{-\infty}^{\infty}U^{(\mathrm{ep})}(\boldsymbol{\rho}',\omega) \times \exp[jk\rho'^2/2z]\exp[-jk\boldsymbol{\rho}\cdot\boldsymbol{\rho}'/z]\mathrm{d}^2\rho'. \tag{3}$$

We assume that the effective beam width is less than the lens radius. This means that we may replace the pupil function $A(\boldsymbol{\rho})$ by unity. On substituting Eq. (2) into Eq. (3), we then find that

$$U(\boldsymbol{\rho},z,\omega) = \frac{\exp[jk\rho^2/2z]}{j\lambda z}e^{jkz}\iint_{-\infty}^{\infty}U^{(\mathrm{in})}(\boldsymbol{\rho}',\omega)\exp[-jk\rho'^2/2f] \times\exp[jk\rho'^2/2z]\exp[-jk\boldsymbol{\rho}'\cdot\boldsymbol{\rho}/z]\mathrm{d}^2\rho'. \tag{4}$$

As is well known, in the special case that $z = f$, Eq. (4) reduces to a Fourier transform relationship, indicating that the lens produces a Fourier transform of the incident beam at its focal plane.

Let us next consider the case where the incident field is an electromagnetic beam. Because we are dealing with a paraxial system, the two transverse Cartesian components of the electric field, E_x and E_y, remain independent and both satisfy Eq. (4). Meanwhile, the axial component E_z is negligibly small and can be ignored.

The second-order statistical properties of a partially coherent beam in a cross-sectional plane z are characterized by the cross-spectral density matrix [16]

$$\mathbf{W}(\boldsymbol{\rho}_1,\boldsymbol{\rho}_2,z,\omega) = \begin{pmatrix} W_{xx} & W_{xy} \\ W_{yx} & W_{yy}\end{pmatrix}. \tag{5}$$

The elements of the matrix are given by the equations

$$W_{ij}(\boldsymbol{\rho}_1,\boldsymbol{\rho}_2,z,\omega) = \langle E_i^*(\boldsymbol{\rho}_1,z,\omega)E_j(\boldsymbol{\rho}_2,z,\omega)\rangle, \quad (i,j = x,y), \tag{6}$$

where the angular brackets denote the average taken over an ensemble of statistical realizations of the beam. For brevity, we will from now on no longer display the dependence of the various quantities on the frequency ω. As both E_x and E_y can be written in the form of Eq. (4), we find that the four elements of the matrix $\mathbf{W}$ evolve with z as

$$W_{ij}(\boldsymbol{\rho}_1,\boldsymbol{\rho}_2,z) = \frac{\exp[jk(\rho_2^2-\rho_1^2)/2z]}{\lambda^2z^2}\iiiint_{-\infty}^{\infty}W_{ij}^{(\mathrm{in})}(\boldsymbol{\rho}_1',\boldsymbol{\rho}_2') \times\exp[-jk(\rho_2'^2-\rho_1'^2)/2f]\exp[jk(\rho_2'^2-\rho_1'^2)/2z] \times\exp[-jk(\boldsymbol{\rho}_2'\cdot\boldsymbol{\rho}_2-\boldsymbol{\rho}_1'\cdot\boldsymbol{\rho}_1)/z]\mathrm{d}^2\rho_1'\mathrm{d}^2\rho_2', \tag{7}$$

where

$$W_{ij}^{(\mathrm{in})}(\boldsymbol{\rho}_1,\boldsymbol{\rho}_2) = \langle E_i^{(\mathrm{in})*}(\boldsymbol{\rho}_1)E_j^{(\mathrm{in})}(\boldsymbol{\rho}_2)\rangle, \tag{8}$$

denote the elements of the cross-spectral density matrix of the incident field. Just as remarked below Eq. (4), when $z = f$, Eq. (7) describes a Fourier transform but now of the elements of the cross-spectral density matrix instead of the field [8].

The degree of polarization depends on the cross-spectral density elements at a single point [see Eq. (16)]. We are therefore concerned with the case $\boldsymbol{\rho}_1 = \boldsymbol{\rho}_2 = \boldsymbol{\rho}$, for which Eq. (7) reduces to

$$W_{ij}(\boldsymbol{\rho},\boldsymbol{\rho},z) = \frac{1}{\lambda^2z^2}\iiiint_{-\infty}^{\infty}W_{ij}^{(\mathrm{in})}(\boldsymbol{\rho}_1',\boldsymbol{\rho}_2')\exp[-jk(\rho_2'^2-\rho_1'^2)/2f]\exp[jk(\rho_2'^2-\rho_1'^2)/2z] \times\exp[-jk\boldsymbol{\rho}\cdot(\boldsymbol{\rho}_2'-\boldsymbol{\rho}_1')/z]\mathrm{d}^2\rho_1'\mathrm{d}^2\rho_2'. \tag{9}$$

For a point of observation in the focal region, we use $z = f + \Delta$ with $|\Delta| \ll f$ in Eq. (9). If we then use the Taylor-series expansion

$$\eta(\Delta) = \frac{1}{f} - \frac{1}{f+\Delta} = \frac{\Delta}{f^2} - \frac{\Delta^2}{f^3} + O(\Delta^3), \tag{10}$$

we can approximate Eq. (9) by the expression

$$W_{ij}(\boldsymbol{\rho},\boldsymbol{\rho},f+\Delta) = \frac{1}{\lambda^2f^2}\iiiint_{-\infty}^{\infty}W_{ij}^{(\mathrm{in})}(\boldsymbol{\rho}_1',\boldsymbol{\rho}_2')\exp\left[-j\frac{k}{2}(\rho_2'^2-\rho_1'^2)\eta(\Delta)\right] \times\exp\left[-j\frac{k}{f+\Delta}\boldsymbol{\rho}\cdot(\boldsymbol{\rho}_2'-\boldsymbol{\rho}_1')\right]\mathrm{d}^2\rho_1'\mathrm{d}^2\rho_2'. \tag{11}$$

This equation can be used to calculate the elements of the cross-spectral density matrix in the focal region. In the next section, we apply it to a wide class of random beams, namely, those of the Gaussian–Schell model [16,19].

3. GAUSSIAN–SCHELL MODEL BEAMS

The elements of the cross-spectral density matrix of the field in the entrance plane can be written as

$$W_{ij}^{(\mathrm{in})}(\boldsymbol{\rho}_1',\boldsymbol{\rho}_2') = \sqrt{S_i^{(\mathrm{in})}(\boldsymbol{\rho}_1')S_j^{(\mathrm{in})}(\boldsymbol{\rho}_2')}\mu_{ij}^{(\mathrm{in})}(\boldsymbol{\rho}_1',\boldsymbol{\rho}_2') \quad (i,j = x,y). \tag{12}$$

Here, $S_i^{(\mathrm{in})}(\boldsymbol{\rho}')$ represents the spectral density of the ith component of the electric-field vector, and $\mu_{ij}^{(\mathrm{in})}(\boldsymbol{\rho}_1',\boldsymbol{\rho}_2')$ is the correlation coefficient between E_i at $\boldsymbol{\rho}_1'$ and E_j at $\boldsymbol{\rho}_2'$. We assume that the lens is situated at the waist plane of a Gaussian–Schell model beam [16]. In that case,

$$S_i^{(\mathrm{in})}(\boldsymbol{\rho}') = A_i^2\exp(-\rho'^2/2\sigma_i^2), \tag{13}$$

$$\mu_{ij}^{(\mathrm{in})}(\boldsymbol{\rho}_1',\boldsymbol{\rho}_2') = B_{ij}\exp[-(\boldsymbol{\rho}_2'-\boldsymbol{\rho}_1')^2/2\delta_{ij}^2]. \tag{14}$$

The parameters A_i, σ_i, B_{ij}, and δ_{ij} are independent of position but may depend on the frequency. They cannot be chosen arbitrarily but have to satisfy several constraints (see Sec. 9.4.2, [16] and [21]). For simplicity, we restrict ourselves to the case where the two spatial widths are identical, i.e.,

$$\sigma_x = \sigma_y = \sigma. \tag{15}$$

The degree of polarization, introduced by Eq. (1), can alternatively be expressed as (Sec. 8.2, [16])

$$P(\boldsymbol{\rho}, z) = \sqrt{1 - \frac{4\mathrm{Det}\, W(\boldsymbol{\rho}, \boldsymbol{\rho}, z)}{[\mathrm{Tr}\, W(\boldsymbol{\rho}, \boldsymbol{\rho}, z)]^2}}, \tag{16}$$

where Det and Tr denote the determinant and trace, respectively. It is easily derived that, in this example, the DOP of the incident beam is independent of position and given by the formula

$$P^{(\mathrm{in})} = \sqrt{1 - \frac{4A_x^2 A_y^2 (1 - |B_{xy}|^2)}{(A_x^2 + A_y^2)^2}}. \tag{17}$$

For the case of $A_x = A_y$, this expression reduces to

$$P^{(\mathrm{in})} = |B_{xy}|. \tag{18}$$

The DOP in the focal region is obtained by calculating the elements of the cross-spectral density matrix there. This is achieved by substituting from Eqs. (13) and (14) into Eq. (11) while introducing sum and difference variables

$$\boldsymbol{R}_+ = \frac{\boldsymbol{\rho}_1' + \boldsymbol{\rho}_2'}{2}, \qquad \boldsymbol{R}_- = \boldsymbol{\rho}_2' - \boldsymbol{\rho}_1'. \tag{19}$$

We then find that the element W_{xx} of the cross-spectral density matrix can be expressed as

$$\begin{aligned} &W_{xx}(\boldsymbol{\rho}, \boldsymbol{\rho} f + \Delta) \\ &= \left(\frac{A_x}{\lambda f}\right)^2 \iint_{-\infty}^{\infty} \exp\left(-\frac{R_+^2}{2\sigma^2}\right) \left\{ \iint_{-\infty}^{\infty} \exp\left(-\frac{R_-^2}{2\Omega_{xx}^2}\right) \right. \\ &\quad \times \exp\left[-jk\boldsymbol{R}_- \cdot \left(\eta(\Delta)\boldsymbol{R}_+ + \frac{\boldsymbol{\rho}}{f + \Delta}\right)\right] \mathrm{d}^2 R_- \left.\vphantom{\iint} \right\} \mathrm{d}^2 R_+, \end{aligned} \tag{20}$$

where we introduced the quantities

$$\frac{1}{\Omega_{ij}^2} = \frac{1}{4\sigma^2} + \frac{1}{\delta_{ij}^2}, \qquad (i, j = x, y). \tag{21}$$

The integrations over $\mathbf{R}_-$ can be carried out analytically to obtain

$$\begin{aligned} &W_{xx}(\boldsymbol{\rho}, \boldsymbol{\rho}, f + \Delta) \\ &= 2\pi \left(\frac{\Omega_{xx} A_x}{\lambda f}\right)^2 \exp[-\gamma_{xx}^2(\Delta)\rho^2] \\ &\quad \times \iint_{-\infty}^{\infty} \exp[-\beta_{xx}^2(\Delta) R_+^2] \exp[-\alpha_{xx}^2(\Delta) \boldsymbol{R}_+ \cdot \boldsymbol{\rho}] \mathrm{d}^2 R_+, \end{aligned} \tag{22}$$

where the new parameters are given by

$$\begin{aligned} &\gamma_{ij}^2(\Delta) = \frac{k^2 \Omega_{ij}^2}{2(f + \Delta)^2}, \qquad \beta_{ij}^2(\Delta) = \frac{1}{2\sigma^2} + \frac{k^2 \Omega_{ij}^2 \eta^2(\Delta)}{2}, \\ &\alpha_{ij}^2(\Delta) = \frac{k^2 \Omega_{ij}^2 \eta(\Delta)}{f + \Delta}. \end{aligned} \tag{23}$$

The last two integrals can be carried out by completing the square in the exponents and making the change of variables

$$\boldsymbol{r}_+ = \beta_{xx}(\Delta)\boldsymbol{R}_+ + \xi_{xx}(\Delta)\boldsymbol{\rho}, \tag{24}$$

where

$$\xi_{ij}^2(\Delta) = \frac{\alpha_{ij}^4(\Delta)}{4\beta_{ij}^2(\Delta)}. \tag{25}$$

The final result is found to be

$$\begin{aligned} &W_{xx}(\boldsymbol{\rho}, \boldsymbol{\rho}, f + \Delta) \\ &= 2\left(\frac{\pi \Omega_{xx} A_x}{\lambda f \beta_{xx}(\Delta)}\right)^2 \exp\{-[\gamma_{xx}^2(\Delta) - \xi_{xx}^2(\Delta)]\rho^2\}. \end{aligned} \tag{26}$$

The other three elements of the cross-spectral density matrix can be calculated in a similar fashion and are given by

$$\begin{aligned} &W_{xy}(\boldsymbol{\rho}, \boldsymbol{\rho}, f + \Delta) \\ &= 2A_x A_y B_{xy} \left(\frac{\pi \Omega_{xy}}{\lambda f \beta_{xy}(\Delta)}\right)^2 \exp\{-[\gamma_{xy}^2(\Delta) - \xi_{xy}^2(\Delta)]\rho^2\}, \end{aligned} \tag{27}$$

$$\begin{aligned} &W_{yx}(\boldsymbol{\rho}, \boldsymbol{\rho}, f + \Delta) \\ &= 2A_x A_y B_{xy}^* \left(\frac{\pi \Omega_{xy}}{\lambda f \beta_{xy}(\Delta)}\right)^2 \exp\{-[\gamma_{xy}^2(\Delta) - \xi_{xy}^2(\Delta)]\rho^2\}, \end{aligned} \tag{28}$$

$$\begin{aligned} &W_{yy}(\boldsymbol{\rho}, \boldsymbol{\rho}, f + \Delta) \\ &= 2\left(\frac{\pi \Omega_{yy} A_y}{\lambda f \beta_{yy}(\Delta)}\right)^2 \exp\{-[\gamma_{yy}^2(\Delta) - \xi_{yy}^2(\Delta)]\rho^2\}, \end{aligned} \tag{29}$$

where in Eq. (28) we made use of the fact that $B_{yx} = B_{xy}^*$ and $\delta_{yx} = \delta_{xy}$ (see Sec. 9.4.2, [16]); hence, $\Omega_{yx} = \Omega_{xy}$, $\gamma_{yx}(\Delta) = \gamma_{xy}(\Delta)$, $\beta_{yx}(\Delta) = \beta_{xy}(\Delta)$, $\alpha_{yx}(\Delta) = \alpha_{xy}(\Delta)$, and $\xi_{yx}(\Delta) = \xi_{xy}(\Delta)$.

In close proximity of the focal plane $\Delta \ll f$, and the factor $\eta(\Delta)$ in Eq. (10) may be well approximated by just a single term of the Taylor series. It then follows that

$$W_{ij}(\boldsymbol{\rho}, \boldsymbol{\rho}, f + \Delta) = W_{ij}(\boldsymbol{\rho}, \boldsymbol{\rho}, f - \Delta), \qquad (i, j = x, y). \tag{30}$$

On making use of Eq. (30) in Eq. (16), one finds that

$$P(\boldsymbol{\rho}, f + \Delta) = P(\boldsymbol{\rho}, f - \Delta). \tag{31}$$

Hence, the degree of polarization in the focal region is symmetric with respect to the focal plane. Furthermore, because the matrix elements depend only on the modulus of the position vector $\boldsymbol{\rho}$, the DOP is also rotationally symmetric around the z axis.

It is instructive to plot the DOP alongside the spectral density

$$S(\boldsymbol{\rho}, z) = W_{xx}(\boldsymbol{\rho}, \boldsymbol{\rho}, z) + W_{yy}(\boldsymbol{\rho}, \boldsymbol{\rho}, z), \tag{32}$$

because the focal region is the volume over which $S(\boldsymbol{\rho}, z)$ is non-negligible. We mention in passing that the definition in Eq. (32) implies that the symmetries of the DOP also apply to the spectral density (c.f. [22,23]).

An example is given by Fig. 1 in which both the spectral density (normalized to unity at the focus) and the DOP are plotted in the focal plane ($z = f$). It is seen that the former decreases monotonically, whereas the latter first decreases and then rises again. The oscillating behavior of the DOP is caused by the different rates with which the different matrix elements W_{xx}, W_{yy}, and W_{xy}, fall off when ρ increases. For values of $\rho > 25$ µm, the W_{xx} element gradually becomes dominant. This means that the field becomes more and more x polarized, leading to an increasing DOP, albeit in a region with a decreasing spectral density. It is important to note that the DOP at the geometrical focus is significantly larger than that of the incident beam, for which $P^{(\mathrm{in})} = 0.3$ for all values of ρ.

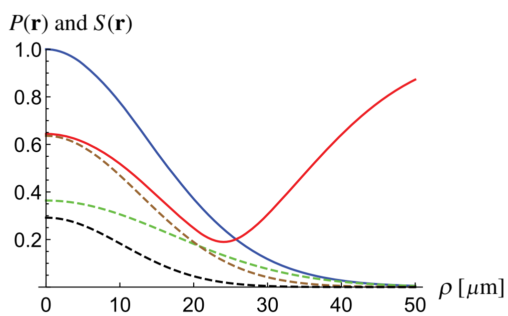

Fig. 1. Normalized spectral density (blue curve) and the degree of polarization (red) in the focal plane ($z = f$). Also shown are W_{xx} (dashed green curve), W_{yy} (dashed brown curve), and W_{xy} (dashed black curve). In this example, $\lambda = 632.8$ nm, $f = 50$ cm, $a = 2$ cm, $A_x = A_y = 1$, $B_{xy} = 0.3$, $\sigma = 10$ mm, $\delta_{xx} = 3$ mm, $\delta_{yy} = 4$ mm, and $\delta_{xy} = 5$ mm.

The DOP and the spectral density along the central axis ($\boldsymbol{\rho} = 0$) are plotted in Fig. 2. Whereas the spectral density decreases to zero when the distance $|\Delta|$ increases, the DOP tends to a constant value, namely, the DOP of the incident field (i.e., $|B_{xy}|$). This value is indicated by the dashed red curve.

The 3D distributions of $S(\boldsymbol{\rho}, z)$ and the DOP in the focal region are shown in Fig. 3. The two quantities show a strikingly different behavior. Because we take the incident field to be a narrow Gaussian beam, rather than a truncated beam with a uniform intensity (as in Sec. 8.8, [1]), no Airy pattern with secondary maxima is expected. Indeed, the spectral density decreases both in the transverse and the longitudinal directions. The DOP, in contrast, has a more complex structure and does not attain its maximum value at the geometrical focus.

It is seen from Eqs. (26)–(29) that the DOP depends on the value of coherence radii δ_{ij} via the parameter $\boldsymbol{\Omega}_{ij}$. This dependence is illustrated in Fig. 4. There, the DOP in the focal plane is plotted for selected values of δ_{xx}, with δ_{xy} and δ_{yy} being kept fixed. Although the general behavior remains the same, it is seen that the DOP at the geometrical focus is considerably higher for the lowest value of δ_{xx} (blue curve). We note that, in all three cases, the DOP at focus is larger than the DOP of the incident field, as indicated by the dashed horizontal line.

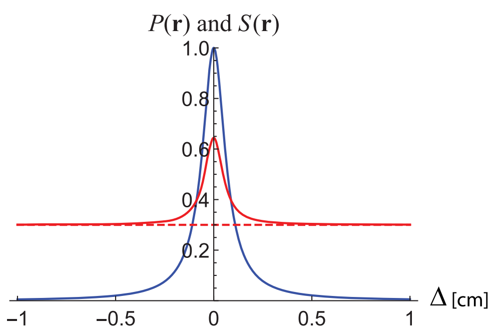

Fig. 2. Normalized spectral density (blue curve) and the degree of polarization (red) along the central axis ($\boldsymbol{\rho} = 0$). The dashed line indicates the value of $P^{(\mathrm{in})}$. Δ denotes the distance from the focal plane $z = f$. The parameters are the same as in Fig. 1.

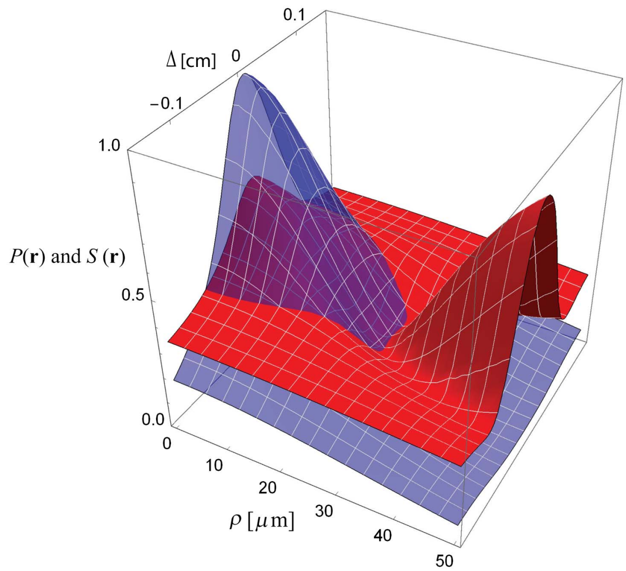

Fig. 3. 3D distribution in the focal region of the spectral density (blue surface) and the degree of polarization (red surface). The parameters are the same as in Fig. 1.

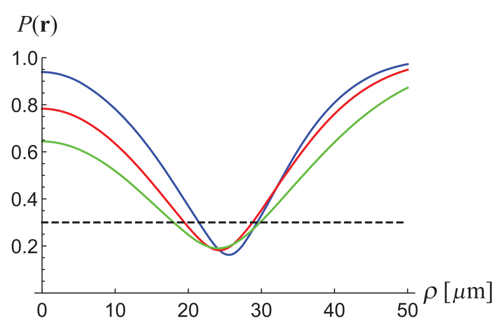

Fig. 4. DOP in the focal plane for selected values of the coherence radius δ_{xx}. Blue curve: $\delta_{xx} = 2.0$ mm; red curve: $\delta_{xx} = 2.5$ mm; green curve: $\delta_{xx} = 3.0$ mm. The DOP of the incident beam is indicated by the dashed black line. All other parameters are as in Fig. 1.

4. CONCLUSIONS

We have used the concept of the cross-spectral density matrix associated with a partially coherent optical beam to show that the degree of polarization across the beam is affected considerably when it is focused by a lens. We use our theory to examine the 3D distribution of the degree of polarization in the focal region of a thin paraxial lens. Our results show that the DOP, a fundamental property of any stochastic wave field, exhibits a complicated behavior. Unlike the spectral density, the maximum value of the DOP need not occur at the geometrical focus. Furthermore, this maximum can be significantly larger than that of the incident beam. These findings may be applied to situations in which the polarization properties of the wave field play a significant role.

Funding. Air Force Office of Scientific Research (AFOSR) (FA9550-16-1-0119); Directorate for Mathematical and

Physical Sciences (MPS) (ECCS-1505636); China Scholarship Council (CSC).

Acknowledgment. TDV's research is supported by the AFOSR; GPA's research is supported by the MPS; X. Z. wishes to thank the CSC.

REFERENCES

1. M. Born and E. Wolf, *Principles of Optics*, 7th ed. (Cambridge University, 1999).
2. H. C. van de Hulst, *Light Scattering by Small Particles* (Dover, 1981).
3. D. F. V. James, "Change of polarization of light beams on propagation in free space," J. Opt. Soc. Am. A **11**, 1641–1643 (1994).
4. O. Korotkova and E. Wolf, "Changes in the state of polarization of a random electromagnetic beam on propagation," Opt. Commun. **246**, 35–43 (2005).
5. O. Korotkova, T. D. Visser, and E. Wolf, "Polarization properties of stochastic electromagnetic beams," Opt. Commun. **281**, 515–520 (2008).
6. T. D. Visser, G. Gbur, and E. Wolf, "Effect of the state of coherence on the three-dimensional spectral intensity distribution near focus," Opt. Commun. **213**, 13–19 (2002).
7. D. G. Fischer and T. D. Visser, "Spatial correlation properties of focused partially coherent light," J. Opt. Soc. Am. A **21**, 2097–2102 (2004).
8. T. D. Visser, G. P. Agrawal, and P. W. Milonni, "Fourier processing with partially coherent fields," Opt. Lett. **42**, 4600–4602 (2017).
9. S. G. Demos and R. R. Alfano, "Temporal gating in highly scattering media by the degree of optical polarization," Opt. Lett. **21**, 161–163 (1996).
10. D. T. Cassidy, S. K. K. Lam, B. Lakshmi, and D. M. Bruce, "Strain mapping by measurement of the degree of polarization of photoluminescence," Appl. Opt. **43**, 1811–1818 (2004).
11. B. Cense, T. C. Chen, B. H. Park, M. C. Pierce, and J. F. de Boer, "In vivo depth-resolved birefringence measurements of the human retinal nerve fiber layer by polarization-sensitive optical coherence tomography," Opt. Lett. **27**, 1610–1612 (2002).
12. R. Shirvany, M. Chabert, and J.-Y. Tourneret, "Ship and oil-spill detection using the degree of polarization in linear and hybrid/compact dual-pol SAR," IEEE J. Sel. Top. Appl. Earth Observ. Remote Sensing **5**, 885–892 (2012).
13. J. Pu and B. Lü, "Focal shifts in focused nonuniformly polarized beams," J. Opt. Soc. Am. A **18**, 2760–2766 (2001).
14. A. L. Sokolov, "Polarization structure of radiation in the focal region of a lens," Opt. Spectrosc. **107**, 207–211 (2009).
15. X. Zhao, T. D. Visser, and G. P. Agrawal, "Controlling the degree of polarization of partially coherent electromagnetic beams with lenses," Opt. Lett. **43**, 2344–2347 (2018).
16. E. Wolf, *Introduction to the Theory of Coherence and Polarization of Light* (Cambridge University, 2007).
17. D. Goldstein, *Polarized Light*, 2nd ed. (Marcel Dekker, 2003).
18. F. Afshinmanesh, J. S. White, W. Cai, and M. L. Brongersma, "Measurement of the polarization state of light using an integrated plasmonic polarimeter," Nanophotonics **1**, 125–129 (2012).
19. L. Mandel and E. Wolf, *Optical Coherence and Quantum Optics* (Cambridge University, 1995).
20. J. W. Goodman, *Introduction to Fourier Optics*, 2nd ed. (McGraw Hill, 1996).
21. F. Gori, M. Santarsiero, R. Borghi, and V. Ramírez-Sánchez, "Realizability condition for electromagnetic Schell-model sources," J. Opt. Soc. Am. A **25**, 1016–1021 (2008).
22. J. J. Stamnes, *Waves in Focal Regions* (IOP, 1986).
23. Y. Chen, J. Gu, F. Wang, and Y. Cai, "Self-splitting properties of a Hermite-Gaussian correlated Schell-model beam," Phys. Rev. A **91**, 013823 (2015).